

Microwave Assisted Green Synthesis of Silver Nanoparticles using Pomegranate Peel Extract: Characterization and Antibacterial Activity Studies

GUGULOTHU YAKU, BANDI RAJKUMAR and T.V.D. PRASAD RAO*

Department of Chemistry, Osmania University, Hyderabad-500007, India

*Corresponding author: E-mail: thyp123@gmail.com

Received: 25 October 2019;

Accepted: 30 November 2019;

Published online: 30 December 2019;

AJC-19742

In the present work, a simple and low cost and eco-friendly technique is applied for the microwave assisted synthesis of silver nanoparticles (AgNPs) using the extract of pomegranate peel wastes, which does not require any use of external stabilizing agent. The extract of pomegranates peelings waste served as a reducing as well as capping/stabilizing agent. The synthesized silver nanoparticles were characterized by using powder X-ray diffraction (XRD), transmission electron microscopy (TEM), FT-IR, UV-visible spectroscopy and scanning electron microscopy-energy dispersive X-ray analysis (SEM-EDX). The stability of AgNPs was analyzed by zeta potential measurements. The antibacterial activity of synthesized AgNPs was also evaluated on six Gram-positive and Gram-negative bacteria using agar well diffusion method.

Keywords: Silver nanoparticles, Pomegranates peel, Microwave irradiation, Antibacterial activity.

INTRODUCTION

Silver nanoparticles (AgNPs) have been used in different fields such as medical, food, health and consumer care industries, *etc.* due to their unique optical, electrical, thermal and biological properties [1-3]. Silver nanoparticles have been employed in biological leveling, biomedical applications [4], many other catalysis, optics, electronics applications [5] and also their applications in medical and pharmaceutical products [6].

The control over the size and size distribution of nanoparticles, can be obtained by changing reducing agents, stabilizers and reaction conditions in synthetic methods, which gives definite catalytic activity for nanoparticles [7-10]. Nanoparticles can be synthesized by using a number of chemical and physical methods, which are hazardous and pollute the environment [1,11-15].

Among the chemical methods, one is using plant extracts as reducing agents and second one is employing biological microorganisms, such as bacteria and fungus as reducing agents [16-19]. Now researchers have to focus on "Green" chemistry and bio-process, in which clean, bio-compatible and ecofriendly process to synthesize nanoparticles [20]. Interestingly, biologically prepared AgNPs shows high yields, solubility and high

stability [1]. The development of AgNPs with controlled structure, such as size, size distribution, shape, surface chemistry, particle morphology and functionality are essential for various biomedical applications [21-27].

Silver nanoparticles are used in biological leveling, since silver exhibits antibacterial activity. The type of reducing agent used in the synthesis of metal nanoparticles determines cytotoxicity, so its characteristic features need to be evaluated before assessing toxicity and biocompatibility [28]. In earlier report [29], silver nanoparticles were synthesized by using sodium borohydride as reducing agent and pomegranate peels extract as stabilizing agent. In the present work, we have synthesized silver nanoparticles by using pomegranate peels extract which can act as both reducing as well as stabilizing agent. To avoid harsh reaction conditions and rapid production of nanoparticles, the microwave irradiation method was selected. At the optimum temperature (600 °C), the physico-chemical and optical properties of synthesized nanoparticles were thoroughly characterized by using various analytical techniques *viz.* UV-visible, FTIR, XRD, SEM-EDX and TEM. The antibacterial activity of synthesized AgNPs was evaluated on both Gram-positive and Gram-negative bacteria using agar well diffusion method.

EXPERIMENTAL

The fresh pomegranate fruit peels were collected from a local fruit market, while the chemicals *viz.* AgNO₃ from Merck and other chemicals/solvents were of analytical grade.

Preparation of pomegranate peel extract: The dried small pieces of pomegranate fruit peels were grounded into fine powder and stored. For the preparation of extract, appropriate amount of pomegranate peels powder was added to deionized water and the solution was stirred for 2 h at 500 rpm. The solution was filtered by using Whatman's filter paper to get a clear and transparent extract. This extract was stored in refrigerator at 4 °C for further usage.

Synthesis of silver nanoparticles: A mixture containing 1 mL of AgNO₃ and 3 mL of pomegranate peelings extract was heated in a microwave oven. The colour of the reaction mixture changed slowly from pale yellow to brown colour, which indicates the formation of AgNPs. The formation of AgNPs are further conformed by UV-vis spectroscopy. The AgNPs were synthesized from reaction mixtures prepared using 0.1 % to 0.5 % concentration of pomegranate peels extract and each mixed with single concentration of AgNO₃ (0.5 % mM) and different concentration of AgNO₃ from 0.1 to 0.5 mM and each mixed with single concentration of extract (0.5 % mM) at different microwave irradiation times from 1 to 10 min.

Characterization: The characterization of synthesized nanoparticles were carried out using various analytical techniques such as UV- visible, FTIR, XRD, Fe-SEM and TEM.

Antibacterial activity: Agar well diffusion assay was performed according to the method described by earlier report [30]. The six pathogens *viz.* *Klebsiella pneumoniae*, *Bacillus subtilis*, *Proteus vulgaris*, *Staphylococcus aureus*, *Pseudomonas aeruginosa* and *Escherichia coli* used in this study were procured from the Department of Microbiology, Osmania University, Hyderabad, India.

RESULTS AND DISCUSSION

In the present work, microwave assisted green method for the synthesis of silver nanoparticles (AgNPs) from AgNO₃ and pomegranate fruit peels extract was carried out by varying synthetic conditions such as concentration of AgNO₃, concentration of extract and at different microwave irradiation times. The microwave is used as energy source, which can increase the rapid production of nanoparticles within few minutes.

UV-visible analysis: The formation of AgNPs can be confirmed by its surface plasmon resonance (SPR) peak at around 420 nm. Fig. 1a shows the absorption spectra of AgNPs synthesized from solutions prepared from different concentrations of extract from 0.1 to 0.5 % mM mixing each with single AgNO₃ concentration (0.5 mM AgNO₃) and microwave irradiation (MWI) time of 10 min. From Fig. 1a, it is evident that with an increase in the concentration of extract, intensity of SPR peak increased gradually and reached to a maximum value at 0.4 %. As SPR peak intensity is directly proportional to the concentration of AgNPs in the solution, an increase in the extract concentration resulted in an increase in the number of AgNPs formation. This is due to the availability of more and more number of polyphenolic compounds with increase in the concentration of extract. However, further increase in the concentration of extract from 0.4 to 0.5 % do not result a significant increase in the formation of AgNPs, which may be due to the reduction of almost all the Ag⁺ ions present in the AgNO₃ solution. Similar results were observed in the case of variation of AgNO₃ concentration.

Fig. 1b shows that the absorption spectra of synthesized AgNPs from solutions using different concentrations of AgNO₃ from 0.1 to 0.5 mM by mixing each with single extract concentration (0.5 %) and MWI time of 10 min. From Fig. 1b, it is evident that with an increase in the AgNO₃ concentration from 0.1 to 0.4 mM, the SPR peak intensity is increased and reaches to maximum. This is due to the addition of more and more number of Ag⁺ into the solution, which are readily undergo reduction by polyphenolic compounds of the extract to produce AgNPs. The unavailability of sufficient amount of reducing molecules (poly phenolic compounds) might be the reason for decrease in the SPR peak intensity at high AgNO₃ concentration (0.5 mM). Finally, microwave irradiation time is optimized by keeping other parameters constant. As shown in Fig. 1c, an increase in the irradiation time also leads to increase in the SPR peak intensities upto 10 min. This is due to the increased thermal energy produced by MWI was absorbed by water molecules. However, further increase in the irradiation time do not improve the number (production) of AgNPs, this may due to the complete reduction of Ag⁺ ions and/or unavailability of polyphenolic compounds, which are responsible for the formation and stabilization of AgNPs [31].

The λ_{\max} and FWHM values at different concentrations of AgNPs are given in Table-1. The biomolecules of pomegranate fruit peels extract clearly shifted the λ_{\max} of absorption spectra

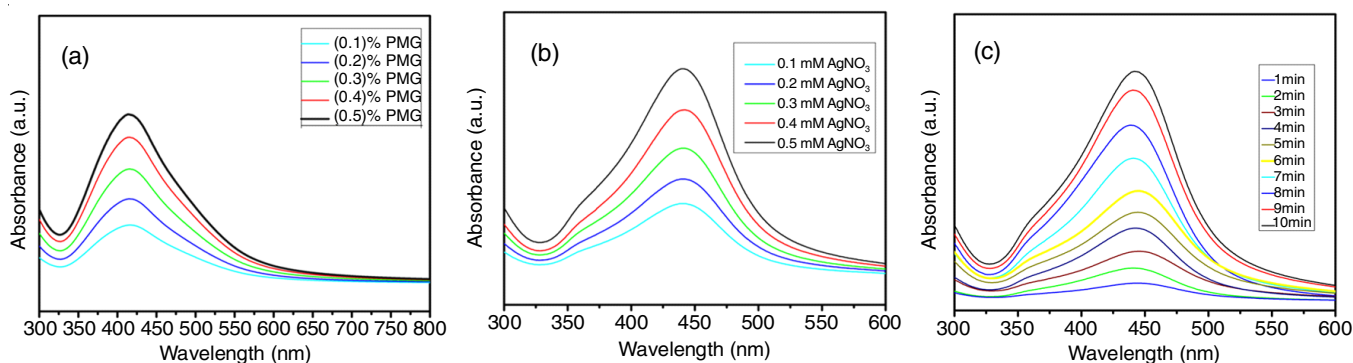


Fig. 1. UV-visible spectra of AgNPs synthesized (a) at different concentrations of pomegranate extract (b) different conc of AgNO₃ and at (c) different time durations

TABLE-1

 λ_{\max} AND FWHM OF DIFFERENT CONCENTRATIONS OF AgNPs WITH 5 % CONCENTRATION OF EXTRACT

Concentration (mM)	λ_{\max} (nm)	FWHM
0.1	440	57
0.2	438	42
0.3	434	40
0.4	430	39
0.5	428	38

of AgNPs. The absorption spectra shifted from 440 to 428 nm (blue shift) with the increase in concentration of AgNPs. The blue shift is due to decrease in the particle size at higher concentration of AgNPs, which results in decreasing the PDI of AgNPs. This may be due to less available number of biomolecules present in fixed concentration of extract (5 %) with increase in concentration of AgNO₃ (0.1-0.5 mM). The FWHM of absorption spectra decreases with the increase in concentration of AgNPs is due decrease in agglomeration of biomolecules of pomegranate peels extract with nanoparticles.

FT-IR analysis: FTIR spectra is recorded in order to provide an evidence for the interaction of functional groups of pomegranate peels extract involved in the reduction of AgNO₃ and the capping of subsequently formed AgNPs. The FTIR spectra of pomegranate peels extract (Fig. 2b) exhibited stretching vibrations at 3400, 2927, 1737, 1328 and 1020 cm⁻¹, while the pomegranate peels extract capped AgNPs shows the characteristic stretching frequencies at 3340, 2953, 1716, 1612, 1340, 1030 cm⁻¹. The broad peak at around 3400 cm⁻¹ corresponds to the O-H stretching vibrations of polyphenols. The peak at around 2900 cm⁻¹ corresponds to C-H stretching and strong peak at around 1700 cm⁻¹ may be assigned to the carbonyl stretching. Further, the peaks at around 1050 cm⁻¹ can ascribe to the C-O stretching. FTIR spectra of pomegranate peels extract capped AgNPs presented some clear distinctions from that of pomegranate peels extract alone. Most importantly, the intensity of O-H stretching vibrations are decreased and the intensity of carbonyl stretching got increased, which suggest that the hydroxyl groups get oxidized to carbonyl groups. This may be due to the reduction of Ag⁺ ions by the hydroxyl groups of polyphenolic compounds, which inturn undergo oxidation [32]. Furthermore, a clear shifts in the peak positions are also observed, which confirms the binding of these functional groups onto the AgNPs.

XRD analysis: The XRD analyses were performed to determine the crystallinity and crystal structure of pomegranate peels extract capped AgNPs. As shown in Fig. 3, four well defined peaks at scattering angles (2θ) of 38.35°, 44.25°, 64.54° and 78.28°. These peaks correspond to the (111), (220), (200) and (311) sets of lattice planes, respectively. These lattice planes confirm the face centered cubic (fcc) crystal structure of the pomegranate peels extract capped AgNPs [33]. A high intense peak was observed for (111) lattice plane and broadening of these peaks suggests the nanosize of the synthesized AgNPs.

SEM-EDX analysis: As shown in Fig. 4a, the SEM image presents the AgNPs with approximately 20 nm in size with nearly spherical morphology. The purity of pomegranate peels extract capped AgNPs and the presence of elemental silver atoms were studied by energy dispersive X-ray analysis. The EDX spectrum

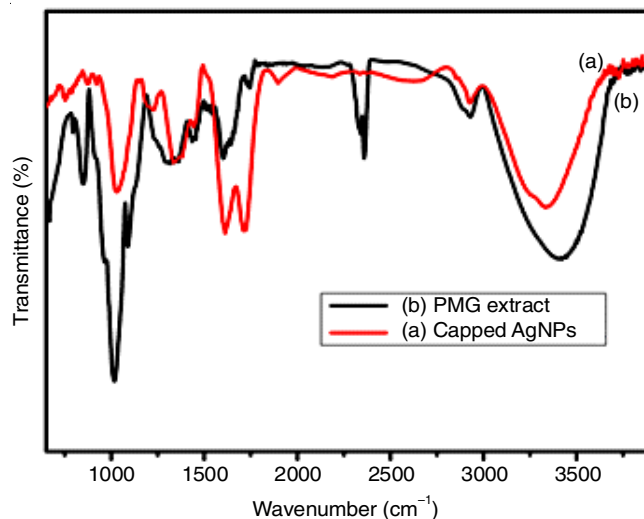


Fig. 2. FTIR spectra of (a) pomegranate capped AgNPs and (b) pomegranate alone

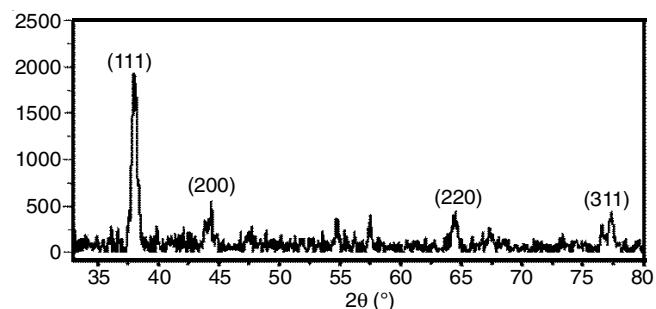


Fig. 3. Powder XRD pattern of pomegranate capped AgNPs

(Fig. 4b) revealed the presence of only carbon, oxygen and silver in pomegranate peels extract capped AgNPs, which implied the purity of formed nanoparticles (C and O were from the extract).

TEM and DLS analysis: TEM analysis (Fig. 5a) was carried out to examine the particle shape and size of the synthesized AgNPs using pomegranate peels extract. TEM morphology shows that the size of AgNPs ranges from 5 to 20 nm and also suggests that synthesized AgNPs were spherical in shape and the average size was 10 ± 2 nm. The selected area electron diffraction pattern (Fig. 5b) exhibited concentric rings with intermittent bright dots indicating that these nanoparticles are highly crystalline in nature.

The effect of different concentration of AgNO₃ on zeta potential, Z-average and PDI of AgNPs are shown in Table-2. The zeta average values are changing from 324.7 to 278.2 d.nm and PDI values are changing from 0.476 to 0.312 in the 0.1 to 0.7 mM concentration range of AgNO₃ indicating that concentration has better control on size and PDI values.

Stability of nanoparticles at different pHs: The colloidal stability of nanoparticles was estimated by zeta size analyzer

TABLE-2

EFFECT OF CONCENTRATION ON ZETA AVERAGE AND PDI

Concentration (mM)	Zeta average (d.nm)	PDI value
0.1	324.7	0.476
0.3	321.2	0.420
0.5	301.2	0.604
0.6	284.9	0.343
0.7	278.2	0.392

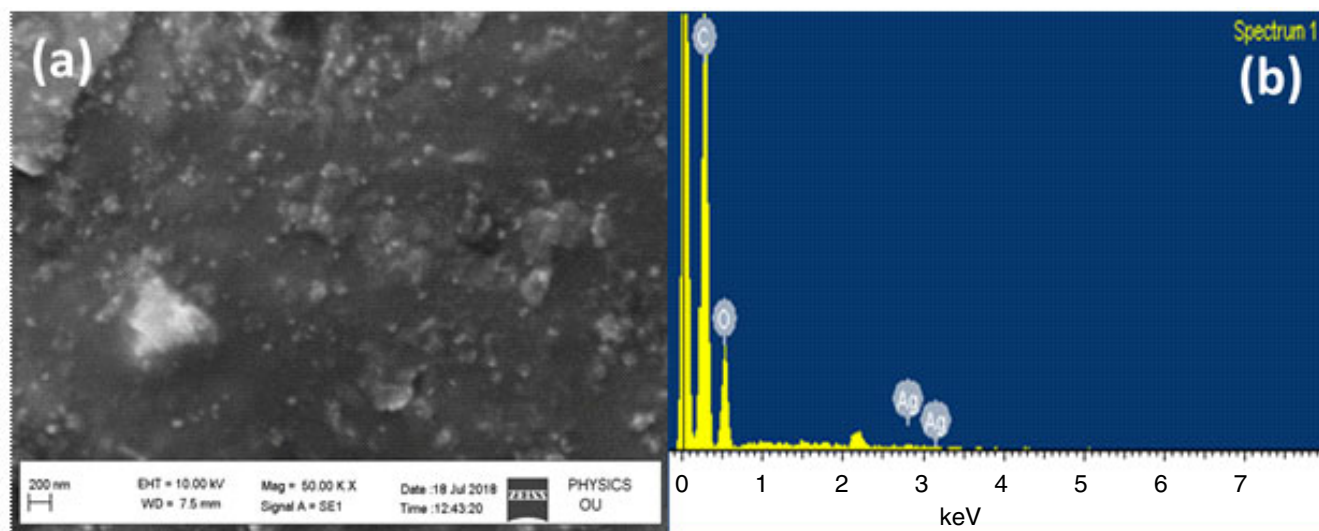


Fig. 4. (a) SEM image of pomegranate capped AgNPs (b) corresponding EDX spectrum

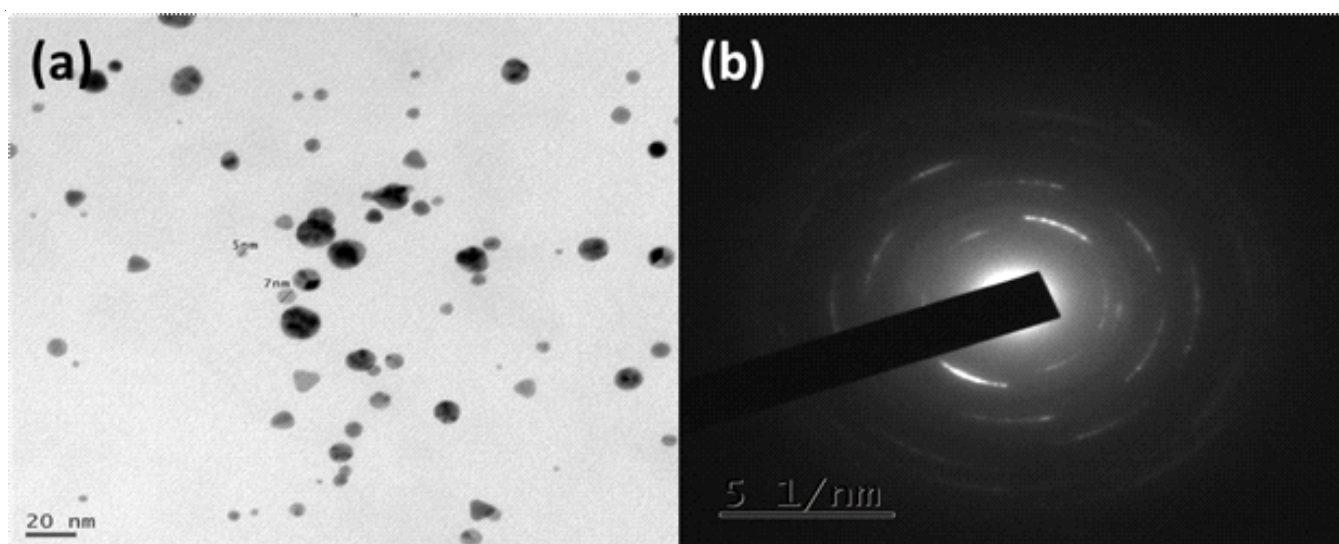


Fig. 5. (a) TEM image of pomegranate capped AgNPs and (b) corresponding SAED pattern

in different pH range from 2 to 11. The results of zeta potential, zeta average and PDI are given in Table-3. It is found that the nanoparticles are stable in the pH range 2-11, as there was less variation in zeta average and zeta potential values. The zeta potential changes from -32.1 to -12.1 mV and zeta average values changing from 299.4 to 219.3 nm in the pH range 2-11. The PDI values were more than 0.7 in the pH range 2-5 indicated the

pH	Zeta average (d.nm)	Zeta potential (mV)	PDI value
2	299.4	-33.2	0.862
3	298.5	-32.1	0.768
4	286.0	-28.5	0.917
5	281.4	25.2	0.730
6	226.4	-15.2	0.472
7	241.3	-13.7	0.568
8	228.5	-13.1	0.365
9	251.5	-12.2	0.347
10	221.4	-11.8	0.331
11	219.1	-11.2	0.312

broad particle distribution. But PDI values were found less than 0.7 in the pH range 6-11, which indicate narrow particle size distribution.

Antibacterial Activity: The antibacterial activity of the pomegranate peels extract capped AgNPs has carried out against six bacteria pathogens viz. *Klebsiella pneumoniae*, *Bacillus subtilis*, *Proteus vulgaris*, *Staphylococcus aureus*, *Pseudomonas aeruginosa* and *Escherichia coli*. The pomegranate peels extract capped AgNPs has shown positive antibacterial activity against *Klebsiella pneumoniae*, *Proteus vulgaris*, *Staphylococcus aureus* and *E. coli* (Table-4) and showed negative antibacterial activity against *Bacillus subtilis* and *Pseudomonas aeruginosa*.

Conclusion

A simple, efficient and eco-friendly synthesis of silver nanoparticles (AgNPs) from the extract of pomegranate peel wastes is reported. The size, PDI, FWHM and colloidal stability of synthesized nanoparticles in dispersion depends on the extract concentration. According to UV-visible studies, the SPR peak intensity are increased with the concentration of extract upto 0.4 %, which indicates the increase in number of nanoparticles

TABLE-4
ZONE OF INHIBITION OF AgNPs IN ANTIBACTERIAL ACTIVITY AGAINST PATHOGENIC BACTERIA

Concentration (mM)	Zone of inhibition (mm)					
	<i>Klebsiella pneumoniae</i>	<i>Bacillus subtilis</i>	<i>Proteus vulgaris</i>	<i>Staphylococcus aureus</i>	<i>Pseudomonas aeruginosa</i>	<i>Escherichia coli</i>
Treptomycin	2.0	0	2.0	1.8	0	1.8
1	1.6	0	1.8	1.8	0	1.8
5	2.0	0	1.6	1.6	0	1.6
10	2.0	0	1.8	1.6	0	1.8

due to increase in number of polyphenolic groups of extract. The rate of formation of nanoparticles increases with the irradiation time upto 10 min. As the concentration of AgNO₃ increases, the Z-average and PDI values decrease, which indicates the concentration has better control on size and PDI values. The synthesized nanoparticles have shown positive antibacterial activity against *K. pneumoniae*, *P. vulgaris*, *S. aureus* and *E. coli*.

ACKNOWLEDGEMENTS

The authors acknowledge DST-FIST, New Delhi for financial support.

CONFLICT OF INTEREST

The authors declare that there is no conflict of interests regarding the publication of this article.

REFERENCES

- S. Gurunathan, J.H. Park, J.W. Han and J.H. Kim, *Int. J. Nanomed.*, **10**, 4203 (2015); <https://doi.org/10.2147/IJN.S83953>.
- W.R. Li, X.B. Xie, Q.S. Shi, H.Y. Zeng, Y.S. Ou-Yang and Y.B. Chen, *Appl. Microbiol. Biotechnol.*, **85**, 1115 (2010); <https://doi.org/10.1007/s00253-009-2159-5>.
- P. Mukherjee, A. Ahmad, D. Mandal, S. Senapati, S.R. Sainkar, M.I. Khan, R. Parishcha, P.V. Ajaykumar, M. Alam, R. Kumar and M. Sastry, *Nano Lett.*, **1**, 515 (2001); <https://doi.org/10.1021/nl0155274>.
- K.M.M. Abou El-Nour, A. Eftaiha, A. Al-Warthan and R.A.A. Ammar, *Arab. J. Chem.*, **3**, 135 (2010); <https://doi.org/10.1016/j.arabjc.2010.04.008>.
- M.S. Akhtar, J. Panwar and Y.S. Yun, *ACS Sustain. Chem. Eng.*, **1**, 591 (2013); <https://doi.org/10.1021/sc300118u>.
- B.H. Kim, M.J. Hackett, J. Park and T. Hyeon, *Chem. Mater.*, **26**, 59 (2014); <https://doi.org/10.1021/cm402225z>.
- S. Yeo, H. Lee and S. Jeong, *J. Mater. Sci.*, **38**, 2143 (2003); <https://doi.org/10.1023/A:1023767828656>.
- J. Zhang, P. Chen, C. Sun and X. Hu, *J. Appl. Catal. A*, **266**, 49 (2004); <https://doi.org/10.1016/j.apcata.2004.01.025>.
- R. Chimentao, I. Kirm, F. Medina, X. Rodriguez, Y. Cesteros, P. Salagre and J. Sueiras, *Chem. Commun.*, **4**, 846 (2004); <https://doi.org/10.1039/B400762J>.
- B. He, J.J. Tan, K.Y. Liew and H. Liu, *J. Mol. Catal. A Chem.*, **221**, 121 (2004); <https://doi.org/10.1016/j.molcata.2004.06.025>.
- S. Gurunathan, K. Kalishwaralal, R. Vaidyanathan, D. Venkataraman, S.R. Pandian, J. Muniyandi, N. Hariharan and S.H. Eom, *Colloids Surf. B Biointerfaces*, **74**, 328 (2009); <https://doi.org/10.1016/j.colsurfb.2009.07.048>.
- J. Sun, D. Ma, H. Zhang, X. Liu, X. Han, X. Bao, G. Weinberg, N. Pfänder and D. Su, *J. Am. Chem. Soc.*, **128**, 15756 (2006); <https://doi.org/10.1021/ja064884j>.
- G. Khomutov and S. Gubin, *Mater. Sci. Eng. C*, **22**, 141 (2002); [https://doi.org/10.1016/S0928-4931\(02\)00162-5](https://doi.org/10.1016/S0928-4931(02)00162-5).
- M. Oliveira, D. Ugarte, D. Zanchet and A. Zarbin, *J. Colloid Interface Sci.*, **292**, 429 (2005); <https://doi.org/10.1016/j.jcis.2005.05.068>.
- E. Egorova and A. Revina, *Colloids Surf. A Physicochem. Eng. Asp.*, **168**, 87 (2000); [https://doi.org/10.1016/S0927-7757\(99\)00513-0](https://doi.org/10.1016/S0927-7757(99)00513-0).
- M. Pileni, *Langmuir*, **13**, 3266 (1997); <https://doi.org/10.1021/la960319q>.
- C. Petit, P. Lixon and M.P. Pileni, *J. Phys. Chem.*, **97**, 12974 (1993); <https://doi.org/10.1021/j100151a054>.
- I. Lisiecki and M. Pileni, *J. Phys. Chem.*, **99**, 5077 (1995); <https://doi.org/10.1021/j100014a030>.
- A. Dokuchaev, T. Myasoedova and A. Revina, *Chem. High Energies*, **31**, 353 (1997).
- G.B. Reddy, A. Madhusudhan, D. Ramakrishna, D. Ayodhya, M. Venkatesham and G. Veerabhadram, *J. Nanostruct. Chem.*, **5**, 185 (2015); <https://doi.org/10.1007/s40097-015-0149-y>.
- A. Panáček, M. Kolár, R. Vecerová, R. Prucek, J. Soukupová, V. Krystof, P. Hamal, R. Zboril and L. Kvítek, *Biomaterials*, **30**, 6333 (2009); <https://doi.org/10.1016/j.biomaterials.2009.07.065>.
- K. Zodrow, L. Brunet, S. Mahendra, D. Li, A. Zhang, Q. Li and P.J. Alvarez, *Water Res.*, **43**, 715 (2009); <https://doi.org/10.1016/j.watres.2008.11.014>.
- K.K. Wong, S.O. Cheung, L. Huang, J. Niu, C. Tao, C.M. Ho, C.M. Che and P.K. Tam, *ChemMedChem*, **4**, 1129 (2009); <https://doi.org/10.1002/cmdc.200900049>.
- S. Gurunathan, K.J. Lee, K. Kalishwaralal, S. Sheikpranbabu, R. Vaidyanathan and S.H. Eom, *Biomaterials*, **30**, 6341 (2009); <https://doi.org/10.1016/j.biomaterials.2009.08.008>.
- M.I. Sriram, S.B.M. Kanth, K. Kalishwaralal and S. Gurunathan, *Int. J. Nanomed.*, **5**, 753 (2010); <https://doi.org/10.2147/IJN.S11727>.
- T. Verano-Braga, R. Miethling-Graff, K. Wojdyla, A. Rogowska-Wrzesinska, J.R. Brewer, H. Erdmann and F. Kjeldsen, *ACS Nano*, **8**, 2161 (2014); <https://doi.org/10.1021/nn4050744>.
- D. Botequim, J. Maia, M.M.F. Lino, L.M.F. Lopes, P.N. Simões, L.M. Ilharco and L. Ferreira, *Langmuir*, **28**, 7646 (2012); <https://doi.org/10.1021/la300948n>.
- C.Y. Li, Y.J. Zhang, M. Wang, Y. Zhang, G. Chen, L. Li, D. Wu and Q. Wang, *Biomaterials*, **35**, 393 (2014); <https://doi.org/10.1016/j.biomaterials.2013.10.010>.
- M. Nasiriboroumand, M. Montazer and H. Barani, *J. Photochem. Photobiol. B*, **179**, 98 (2018); <https://doi.org/10.1016/j.jphotobiol.2018.01.006>.
- T.R. Lakshmeesha, M.K. Sateesh, B.D. Prasad, S.C. Sharma, M. Kavyashree, M. Chandrasekhar and H. Nagabhushana, *Cryst. Growth Des.*, **14**, 4068 (2014); <https://doi.org/10.1021/cg500699z>.
- V.V. Makarov, A.J. Love, O.V. Sinityna, S.S.I.V. Makarova, M.E. Yaminsky, Taliansky and N.O. Kalinina, *Acta Naturae*, **6**, 35 (2014); <https://doi.org/10.32607/20758251-2014-6-1-35-44>.
- B.R. Gangapuram, R. Bandi, M. Alle, R. Dadigala, G.M. Kotu and Guttena, *J. Mol. Struct.*, **1167**, 305 (2018); <https://doi.org/10.1016/j.molstruc.2018.05.004>.
- S. Rajput, R. Werezuk, R.M. Lange and M.T. Mcdermott, *Langmuir*, **32**, 8688 (2016); <https://doi.org/10.1021/acs.langmuir.6b01813>.